Journal of Academia Vol. 10, Issue 2 (2022) 175 – 186

A PRELIMINARY INVESTIGATION OF POLYANILINE/CHITOSAN COMPOSITE'S PHYSICOCHEMICAL PROPERTIES AND POTENTIAL ELECTROCHEMICAL APPLICATION

Nur Farahin Suhaimi[1], Siti Nor Atika Baharin[2], Nurul Ain Jamion[2], Kavirajaa Pandian Sambasevam[2,3]*

[1]*Faculty of Applied Sciences, Universiti Teknologi MARA, 40450, Shah Alam, Selangor, Malaysia*
[2]*Advanced Materials for Environmental Remediation (AMER), Faculty of Applied Sciences, Universiti Teknologi MARA, Cawangan Negeri Sembilan, Kampus Kuala Pilah, 72000, Negeri Sembilan, Malaysia*
[3]*Electrochemical Material and Sensor (EMaS) Research Group, Universiti Teknologi MARA, 40450 Shah Alam, Selangor, Malaysia*

[*]*Corresponding author: kavirajaa@live.com*

Abstract

A polyaniline/chitosan (PANI/CHT) modified SPCE based sensor was developed and validated by electrochemical detection of PFOA. The PANI/CHT composite was synthesized by chemical oxidative polymerization technique. The synthesized material was characterized by scanning electron microscope (SEM)-Energy dispersive X-ray spectroscopy (EDX), Thermal gravimetric analysis (TGA) and Ultraviolet visible Spectroscopy (UV-Vis) techniques. Therefore, from the SEM result showed that the combination of both materials give porous morphology which would further enhance the electrochemical activity of PANI-CHT composite against PFOA. From the TGA analysis also revealed that the addition of CHT to the PANI would increase the thermal stability of the composite compared to the PANI. In addition, the redox properties of the modified SPCE were examined by cyclic voltammetry studies. The investigation showed that PANI/CHT SPCE exhibit high electroactive surface area compared to unmodified SPCE. The PANI/CHT SPCE recorded lowest detection limit (LOD) of 1.60 ppb with LOQ of 4.82 ppb, in the linear range of 25-50 ppb.

Keywords: Polyaniline, Chitosan, Perfluorooctanoic acid, Screen-Printed Carbon Electrode, Electrochemical Sensor.

Article History:- Received: 16 August 2022; Revised: 25 August 2022; Accepted: 27 August 2022; Published: 31 October 2022

Introduction

Perfluorooctanoic acid (PFOA) is a synthetic perfluorinated compound (PFCs) and known as common emerging environmental contaminants (Dewitt et al., 2012). The contamination of PFOA has received considerable attention over the years and pose a major health concern including certain types of cancers, cardiovascular problems and birth defects (Atsdr, 2004). The unique properties of the PFOA is the carbon fluorine (C–F) bonds which is strongest covalent bond in organic chemistry (485 kJ/mol) that attribute to its high thermal and chemical stability (Ordonez et al., 2022). Hence, it is extremely hard to undergo degradation processes, such as biodegradation and chemical oxidation. It was used in several domestic and industrial applications, and as a consequence of its use, PFOA was widely detected in various water matrices, wildlife and even human blood throughout the world (Ahrens & Bundschuh, 2014; Shankar et al., 2012). Therefore, owing to the strong (C-F) bond, high electronegativity, smaller size of the fluorine atom makes them stables to travel for long distances in a natural environment (Sznajder-Katarzyńska et al., 2019). Therefore, the U.S. Environmental Protection Agency (EPA) announced the lifetime health advisory level of PFOA in drinking water to be 70 ng/L or 70 ppt (Cordner et al., 2019; EPA, 2016). Thus, there is a need to fabricate easy and cost-effective techniques for the fast and reliable measurement of PFOA. Frequently used analytical methods used for validation of PFOA, includes chromatographic technique; high performance liquid chromatographic (HPLC) and liquid chromatography–tandem mass spectrometry (LC–MS/MS) However, these techniques require complex instrumentation, have tedious sample pre-treatment process, and expensive making them

inapplicable for on-site measurements (Ryu et al., 2021). Thus, electrochemical methods have been reported to possess unique advantages, such as cost-effectiveness, convenience for onsite application, ease of use, easier construction of electrode materials, and rapid response during analysis (Younis et al., 2021). In light of this, one of the most up-to-date research has focused on the development a simple, cost-effective, and selective electrochemical sensor that comprised of screen-printed carbon electrodes (SPCE) which small in size, simple and have a high conductivity due to the carbon paste used during the printing process (Padmalaya et al., 2022). However, further modification of the electrode surface is required to improve its performance in sensor. Poly-aniline (PANI) is the most promising conducting polymers (CPs) that exhibit many remarkable properties; such as conductivity, thermal and chemical stability (Anisimov et al., 2020). Due to several advantages, it has been effectively utilized in numerous sensors and exhibited excellent sensitivity and low detection limit (Che et al., 2019; Faisal et al., 2020; Suhail et al., 2019). Nevertheless, based on the previous studies on PANI-based sensors, it showed low mechanical properties that limit its functionality, electronic interactions and current flow. In this work, a rather eco-friendly, chitosan (CHT) was integrated with PANI to modify the SPCE surface for electrochemical determination of PFOA. CHT, as a natural cationic biopolymer, owing to its unique characteristics features such as good water permeability, high adhesion ability, film-forming ability, high mechanical strength, biocompatibility and nontoxicity (Mittal et al., 2018). The use of CHT can improve the stability of the electrode surface by forming a film on the electrode surface. In our research, the electrochemical behavior properties using PANI/CHT composite has been studied. PANI/CHT composite has been synthesized through chemical oxidative polymerization technique. As far as we know, the development of modified SPCE with PANI-CHT composite for the detection of PFOA is still not available in the literature. Functionalizing the electrode surface with the PANI/CHT tends to improve the additional features that can enhance the electrochemical behavior for PFOA detection. Reactive groups in CHT will speed up the transfer of electrons, resulting in more effective electrochemical sensing. The drop-casting method has been used to modify electrode surfaces since it is an efficient and straightforward method. The electrochemical characterization and behavior of the modified-SPCE were investigated using UV-VIS, SEM-EDX, TGA and CV.

Methods

Chemicals and Materials

In this study, aniline (99% purity), ammonium peroxydisulfate (APS), and hydrochloric acid (HCl, 37%) were purchased from R&M, while sodium hydroxide (NaOH, 50%) was obtained from Sigma Aldrich for the extraction of CHT from Crab Shells (CS). The supporting electrolytes, such as potassium chloride (KCl), potassium ferricyanide ($K_3[Fe(CN)_6]$), and dimethyl sulfoxide (DMSO, 99%), were supplied by Fisher Scientific. The analyte, such as perfluorooctanoic acid (PFOA, 95%), was purchased from Sigma-Aldrich. Deionised (DI) water was used for the dissolution of other chemical substances. All reagents were of analytical grade (*A.R.*) unless specified differently.

Synthesis of PANI/CHT composite *via* Chemical Oxidative Polymerization

Dry CHT was first dissolved in 2% acetic acid solution at a weight to volume (w/v) ratio of 1:10 for 24 hrs to form a colourless homogenous aqueous solution. In the resultant solution, 15 mM aniline monomer in 100 mL of 1.0 M HCl was added under constant stirring at 600 rpm for an hour. Then, 15 mM APS solution was added drop-by-drop into the solution under pre-cooled conditions for an hour and constant stirring at 600 rpm. Finally, the *in-situ* polymerisation of PANI-CHT was carried out for 24 hrs at 0 °C. PANI was also synthesised in the absence of CHT as a control in the study.

Modification of Electrode Surface (SPCE)

For the surface modification, the electrode surface was rinsed with deionized water to remove any impurities/dust presence on SPCE. Then, the SPCE was modified through the addition of 1.0 μL of PANI by drop-casting technique and this procedure was repeated for the remaining material (CHT and PANI/CHT composite). Then, the modified SPCEs were dried at RT for a week in a petri dish filled with silica gel to evaporate the residual solvent.

Characterization and Electrochemical Measurement

The modified-SPCE with CHT, PANI, and PANI-CHT composites were characterised by using various methods such as Ultraviolet-Visible (UV-vis), Scanning Electron Microscopy (SEM), Energy Dispersive X-Ray (EDX) analysis and Thermal Gravimetric Analysis (TGA). In this study, the electrochemical characterisation and testing of the sensor were performed *via* CV using AUTOLAB potentiostat/galvanostat (PGSTAT204) (Metrohm). The CV experiment of the modified SPCEs were conducted between -1.0 V and +1.0 V at a scan rate of 100 mV/s in 1.0 mM $K_3[Fe(CN)_6]$ solution containing 1.0 M KCl as the probe. Additionally, the electrochemical behaviour effect of the scan rate and pH of the modified SPCE was determined using the CV method in the presence of 25 ppb PFOA in 0.2 M Phosphate Buffer Solution (PBS).

Results and Discussion

Physicochemical Analysis

Figure. 1 (a), (b) and (c) depicts the SEM micrographs of the CHT, PANI and PANI/CHT composite at 10k magnification. It was observed that the CHT appeared to smooth, irregular and thick surface structure (Geetha Devi et al., 2012), while the thin-film PANI exhibited a cauliflower-like structure with a highly porous texture (Fahim et al., 2019). In contrast, the morphology of the PANI/CHT composite in Figure. 1(c) illustrates the porous structures with the presence of cavity that leads to improvement in ion transportation and electron transfer in conductive material during the charge-discharge process (Waikar et al., 2020). Besides, the EDX analysis was performed to explore the elemental compositions on the surface of the materials, as shown in Figure 1. Based on the results, the Carbon, Oxygen, Nitrogen, and Sulphur element are present in the CHT, PANI, and PANI-CHT composite and the summary of the elemental distribution of the samples are provided in the Table 1. The Sulphur (S) was presented in the EDX spectra, which most likely originated from APS as the oxidant in the polymerisation process (Karthik & Meenakshi, 2015).

Table 1. Summary of elementary EDX analysis for the synthesis materials.

% Wt.	N	O	C	S	F
CHT	14.23	32.31	53.46	-	-
PANI	22.13	10.10	67.06	0.72	-
PANI-CHT	16.46	13.26	65.63	4.66	

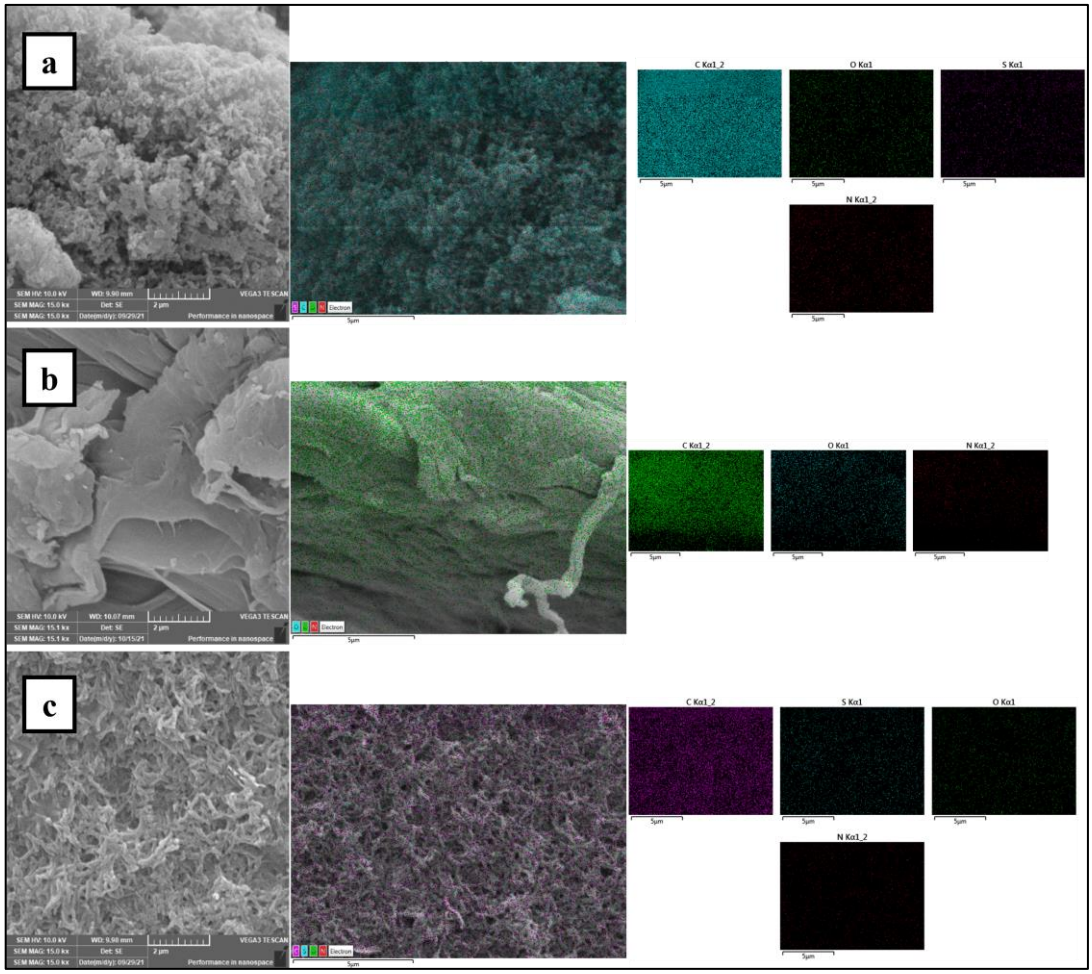

Figure 1. SEM-EDX mapping at 10kx magnification of PANI, CHT and PANI/CHT composite

The TGA was used to determine the thermal stability of the synthesized PANI-CHT composites and compared to that of the CHT and PANI as shown in Figure 2. According to the results, CHT and PANI exhibited two and three sequential decomposition steps, respectively. The first weight loss was recorded at a range of 60–86 °C for all materials, which indicated the evaporation of moisture/water and any unreacted species. For the CHT, the second weight loss was observed at a range of 440-525 °C, which was associated with the degradation of glycosidic bonds within the polysaccharide rings and deacetylated chains with a total residue of 65.88% (Cabuk et al., 2014). Meanwhile, the second and third weight losses for the PANI were recorded at a range of 243–353 °C and 350–550 °C with a weight loss of approximately 52.97% and 22.04%, respectively, and a total residue of 15.1%. The summary of TGA analysis has been provided in Table 2. These occurrences were ascribed to the phase transition and the decomposition of the PANI backbone (Sahnoun & Boutahala, 2018). In comparison, CHT exhibited higher thermal stability than PANI since PANI lost more weight than CHT. In addition, it was assumed that the presence of CHT enhanced the thermal stability of the composite due to the intermolecular and intramolecular hydrogen bonding in the composite structure (Huang et al., 2021).

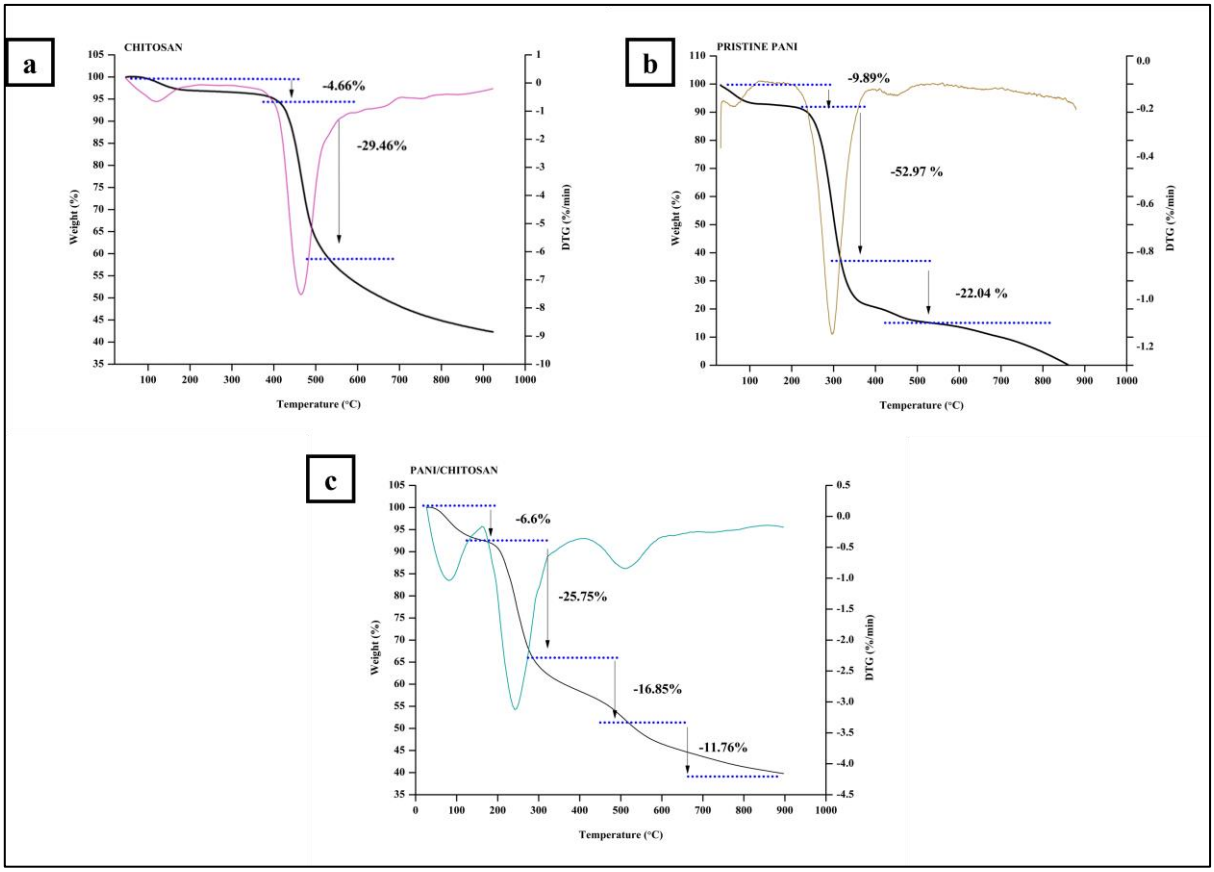

Figure 2. Thermal stability profile for the synthesized materials

Table 2. Summary of TGA analysis for the synthesized materials.

Materials	T_{onset} (°C)	T_{endset} (°C)	T_{max} (°C)	1st weight loss (%)	2nd weight loss (%)	3rd weight loss (%)	4th weight loss (%)	Total residue (%)
CHT	252.79	510.64	467.45	4.66	29.46	-	-	65.88
PANI	235.35	319.54	298.76	9.89	52.97	22.04	-	15.1
PANI-CHT	176.24	276.50	236.97	6.6	25.75	16.85	11.76	39.04

The UV-vis spectra of CHT, PANI, and PANI-CHT composite are shown in Figure 3. According to the CHT spectra, a characteristic band was detected at 264 nm, which corresponds to the π–π∗ transition. However, Thamilarasan *et al*., 2018 stated that this band belongs to the unsaturated bond on the covalent linkage (glucosamine unit) in the CHT structure (Thamilarasan et al., 2018). Oppositely, three significant bands at 325 nm, 480 nm, and 634 nm in the pristine PANI were attributed to the π–π∗, polaron–π∗, and π–polaron, respectively, where the peak at 325 nm was assigned to the benzenoid ring (Mohd Norsham et al., 2020). In addition, a small shoulder polaron band at 480 nm signifies the conductive nature of PANI, which can only be observed in emeraldine salt (Dhivya et al., 2019; Goswami et al., 2016). Meanwhile, the band at 634 nm was attributed to the doped state of PANI. Thus, the detected absorption band at 275 nm confirmed the presence of CHT in each PANI-CHT composite, which corresponds to π–π∗. Furthermore, the bathochromic shift and hypsochromic shift were observed at 380 nm and 457 nm, respectively, with the addition of CHT in the PANI due to the interaction of the glucopyranose component in CHT with the electronic transition of benzenoid and quinoid rings (Cabuk et al., 2014). Therefore, the shifting might be occur due to the absorption and the bond formation between the amine group of PANI on the surface of CHT (Mostafaei & Zolriasatein, 2012).

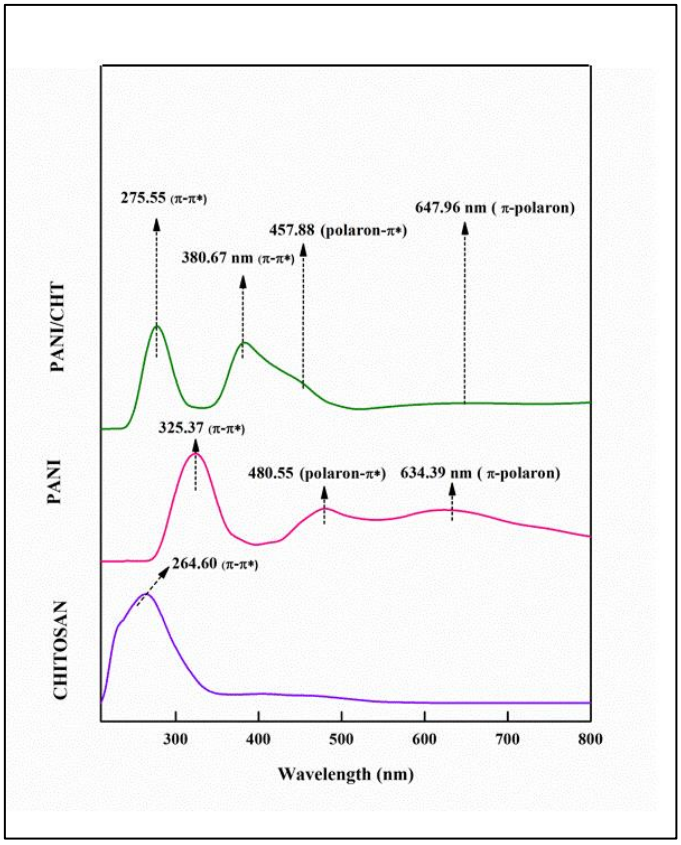

Figure 3. UV-Visible pattern of PANI, CHT and PANI/CHT Composite

Electrochemical Performance of potassium ferrocyanide, $K_3[Fe(CN)_6]$ at the modified SPCE

The cyclic voltammetry (CV) response of the BARE, PANI, CHT and PANI/CHT SPCE were studied in 1.0 mM $K_3[Fe(CN)_6]$ containing 1.0 M potassium chloride (KCl) solution at the scan rate of 100 mVs^{-1} as shown in the Figure 4. The CV indicates a well-defined redox peak for the PANI and PANI/CHT SPCE. However, there is no redox signal for CHT SPCE since it is non-conductive material (Nontipichet et al., 2021). From the studies, the redox peak data for the modified SPCE are shown in Table 3. The redox peak current ratio (I_{pa}/I_{pc}) for PANI/CHT SPCE was higher than the PANI/SPCE. This phenomenon suggests an enhancement in the current signal of the PANI/CHT SPCE are due to the cationic nature on the protonated C2 (amino groups) in CHT and the electron conducting behaviour on the conjugated structure of the PANI salt itself enhanced the electron transfer (Figiela et al., 2018; Rajeev et al., 2020) Therefore, the Electroactive surface area (EASA) of the electrode was calculated by using the Randles-Sevcik equation 1 (Ferrari et al., 2018). The EASA of the PANI and PANI/CHT SPCE was 0.121 cm^2 and 0.137 cm^2 correspondingly, and it indicates the PANI/CHT SPCE has high EASA as compared to PANI SPCE due to the synergistic effect obtained from the excellent electrical conductivity of PANI and the high electrocatalytic active sites of CHT. This finding was supported by the SEM morphology of the PANI/CHT composite, which revealed a porous structure with a cavity that facilitates the electron transfer process (Nontipichet et al., 2021). Therefore, these parameters make the PANI/CHT SPCE more suitable for redox application than the PANI SPCE.

$$I_p = 2.69 \times 10^5 \mathrm{A} \times \mathrm{D}^{1/2} \mathrm{n}^{3/2} \mathrm{v}^{1/2} \mathrm{C} \quad (1)$$

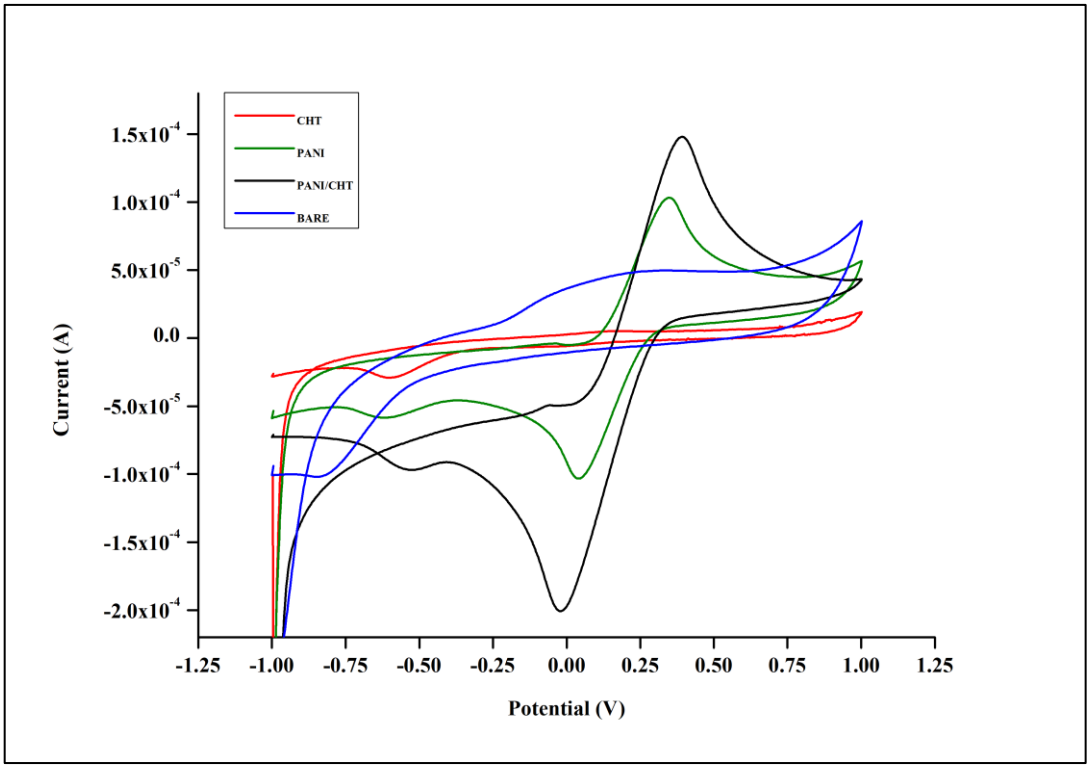

Figure 4. CV response of BARE, PANI, CHT and PANI/CHT SPCE in the 1.0 mM $K_4[Fe(CN)_6]$ at scan rate of 50mVs^{-1}

Table 3. The CV redox for 1.0 mM $[Fe(CN)6]^{4-}$ containing 1.0 M KCl at the SPCEs at scan rate: 100 mVs^{-1}

Electrode	I_{pa}(A)	E_{pa}(V)	I_{pc}(A)	E_{pc}(V)	E^o(V)	I_{pa}/I_{pc}	ΔE_p(V)
Bare	-	-	-	-	-	-	-
CHT	-	-	-	-	-	-	-
PANI	1.26×10^{-4}	0.41595	-1.93×10^{-4}	-0.10895	0.15	0.65	0.31
PANI/CHT	1.79×10^{-4}	0.43304	-2.32×10^{-4}	-0.04303	0.20	0.77	0.40

Electrochemical behaviour of PFOA at PANI/CHT SPCE

Figure 5 (a) shows electrochemical CV response of PANI/CHT in the absence and presence of 25 ppb PFOA in 0.25 M PBS, pH 7.2 with a scan rate at 50mVs^{-1}. As shown in the figure, the CV response for PANI/CHT SPCE (black line) with the absence of PFOA show low redox current signal. However, the CV response was enhanced with the presence of PFOA at the PANI/CHT SPCE (red line) in the oxidation and reduction peak current. The redox peak potential of PANI/CHT SPCE shows redox peak potential at Epa: 0.567 V and Epc: -0.155 V respectively with the change in peak potential of 0.722 V, it implies that higher the electron transfer rate as the change in peak potential is lower (Núñez et al., 2021). The above results are indicates the electrocatalytic activity of PANI/CHT SPCE during the detection of PFOA (Priyanka & Latha, 2021). The scan rate variation from 20-100 mVs^{-1} for PANI/CHT SPCE were studied in 0.25 M PBS, pH 7.2 as shown in the Figure 5 (b). Both oxidation and reduction peak current increases with increasing the scan rate and the oxidation peak potential shift to less negatively and reduction peak current shift to less positively. Therefore, the electrochemical oxidation and reduction of CV response on PANI/CHT SPCE were investigated by different concentration PFOA (25-50 ppb) in pH 7.2 of 0.25 M PBS at scan rate of 50 mVs^{-1}. Figure 5 (c) signifies that the concentration of PFOA increases with redox peak current also increases. Thus, the graph of Ipa vs PFOA concentration was plotted and present a straight line with good linearity as shown in the Figure 5 (d). The limit of detection (LOD) of the sensor was calculated to be 1.60 ppb using the formula, LOD = 3S/m, where S is the standard deviation, m is the slope of the calibration curve and 3 being the signal to noise ratio. Remarkably, our modified electrode can be considered more reliable than the other sensor

as reported in the Table 4. The measured LOD was 1.60 ppb and can be considered more feasible compared to the fluorescence and optical signal. In comparison, the LOD for ion selective electrode is 1ppb which very competitive to our recorded LOD however, PANI/CHT SPCE has recorded the fastest detection time which is <5 min which is significant to be a quick detector. In view of the simple electrode fabrication process, instant detection time and low detection limit, the present work suggests that the PANI/CHT SPCE is a promising electrode sensor that can be used to monitor the presence of PFOA in environmental water samples.

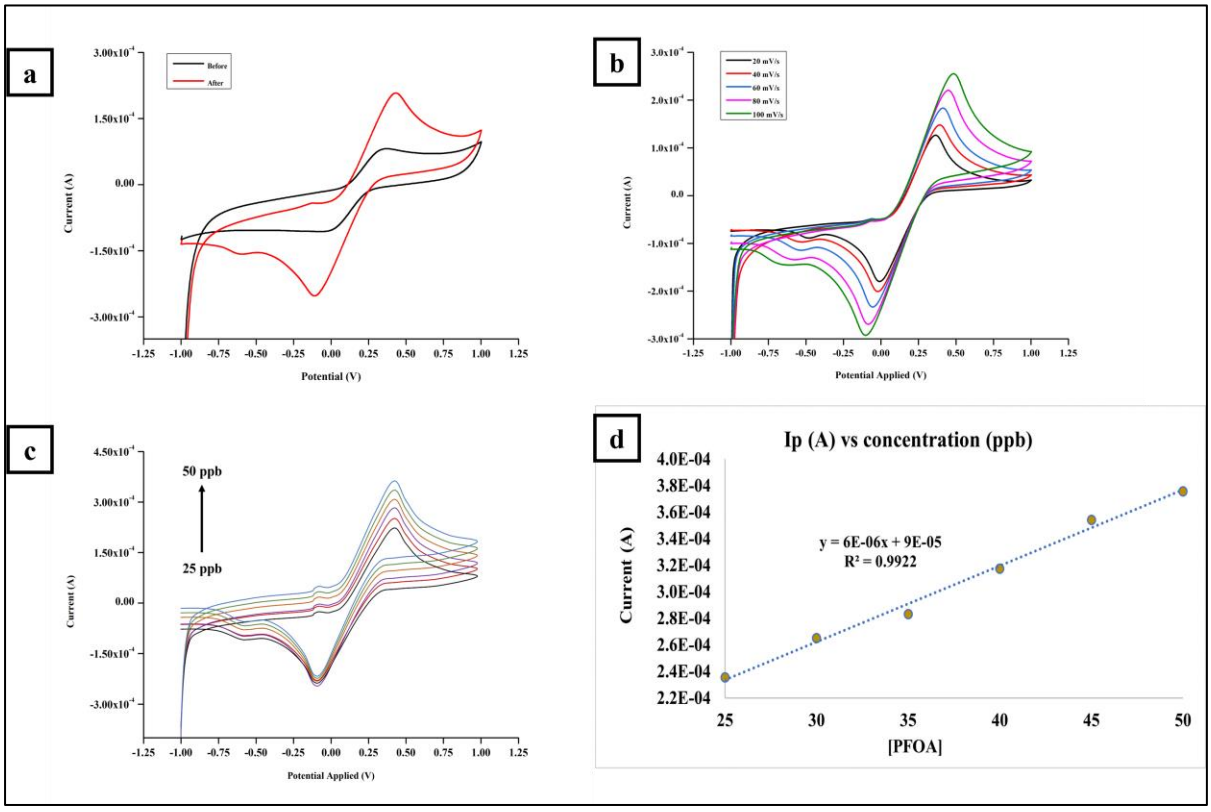

Figure 5. (a) CV responses of PANI/CHT SPCE - absence of PFOA (black line) and PANI/CHT SPCE – (red line) in the presence of 25 ppb PFOA in 0.25 M PBS at pH 7.2, scan rate: 50 mVs^{-1} (b) CV of different scan rate in the presence of 25 ppb PFOA. Scan rate: 20-100 mVs^{-1} (c) CV response for PANI/CHT SPCE with a range of PFOA concentration from 25-50 ppb (d) Calibration curve for different PFOA concentration

Table 4. Comparison table of PFOA detection with different detection method

Platform Material	Method of Detection	LOD (ppb)	Time (min)	Reference
[a]Magnetic Fe_2O_3 NPs	Fluorescence signal	10.9 ± 0.1	15 min	(Zheng et al., 2019)
[b]FPI optical fiber	Optical signal	5	[f] n.r	(Faiz et al., 2020)
IS electrode	Potentiometric signal	1	2880	(Chen et al., 2013)
[c] Pt nanoelectrode	(HER)	30	[f] n.r	(Ranaweera et al., 2019)
[d]SPCE	Voltammetric signal	1.60	< 5	This work

[a] Magnetic Iron Oxide Nanoparticles
[b] Fabry-Perot Interferometry optical fiber
[c] Platinum nanoelectrode
[d] Screen printed carbon electrode
[e] Hydrogen Evolution Reaction
[f] Not reported

Conclusion

In summary, we have demonstrated a facile, chemical oxidative polymerization synthesis of PANI/CHT composite that was drop cast onto the SPCE for the first ever sensing of PFOA. Detection of PFOA was performed using CV technique. The sensor demonstrated very low LOD of 1.60 ppb in a linear range of 25-50 ppb. The PANI/CHT SPCE developed in this work can be used to develop similar electrochemical sensors for various potential hazardous analyte.

Acknowledgement/Funding

The authors would like to show high gratitude to the Fundamental Research Grant Scheme (FRGS) [FRGS/1/ 2019/WAB05/UITM/02/5] for the financial assistance to complete this project.

Author Contribution

NF Suhaimi – Fomal analysis, investigation; SNA Baharin – Supervision, Writing – Review & Editing; NA Jamion - Supervision, Writing – Review & Editing; KP Sambasevam – Supervision, Writing – Review & Editing.

Conflict of Interest

The authors declare that they have no known competing financial interests or personal relationships that could have appeared to influence the work reported in this paper.

References

Ahrens, L., & Bundschuh, M. (2014). Fate and effects of poly- and perfluoroalkyl substances in the aquatic environment: A review. *Environmental Toxicology and Chemistry*, *33*(9), 1921–1929. https://doi.org/10.1002/etc.2663

Anisimov, Y. A., Cree, D. E., & Wilson, L. D. (2020). Preparation of Multicomponent Biocomposites and Characterization of Their Physicochemical and Mechanical Properties. *Journal of Composites Science*, *4*(1), 18. https://doi.org/10.3390/jcs4010018

Agency for Toxic Substances and Disease Registry (Atsdr) (2004). *Chlordane Chapter 2 . Health Effects*. 21–449. https://www.atsdr.cdc.gov/toxprofiles/tp31.pdf. [Access online 21 October 2022].

Cabuk, M., Yavuz, M., & Unal, H. I. (2014). Electrokinetic properties of biodegradable conducting polyaniline-graft-chitosan copolymer in aqueous and non-aqueous media. *Colloids and Surfaces A: Physicochemical and Engineering Aspects*, *460*, 494–501. https://doi.org/10.1016/j.colsurfa.2014.02.053

Che, B., Li, H., Zhou, D., Zhang, Y., Zeng, Z., Zhao, C., He, C., Liu, E., & Lu, X. (2019). Porous polyaniline/carbon nanotube composite electrode for supercapacitors with outstanding rate capability and cyclic stability. *Composites Part B: Engineering*, *165*, 671–678. https://doi.org/10.1016/j.compositesb.2019.02.026

Chen, L. D., Lai, C. Z., Granda, L. P., Fierke, M. A., Mandal, D., Stein, A., Gladysz, J. A., & Bühlmann, P. (2013). Fluorous membrane ion-selective electrodes for perfluorinated surfactants: Trace-level detection and in situ monitoring of adsorption. *Analytical Chemistry*, *85*(15), 7471–7477. https://doi.org/10.1021/ac401424j

Cordner, A., De La Rosa, V. Y., Schaider, L. A., Rudel, R. A., Richter, L., & Brown, P. (2019). Guideline levels for PFOA and PFOS in drinking water: the role of scientific uncertainty, risk assessment decisions, and social factors. *Journal of Exposure Science and Environmental Epidemiology*, *29*(2), 157–171. https://doi.org/10.1038/s41370-018-0099-9

Dewitt, J. C., Peden-Adams, M. M., Keller, J. M., & Germolec, D. R. (2012). Immunotoxicity of Perfluorinated Compounds: Recent Developments. *Toxicologic Pathology*, *40*(2), 300–311. https://doi.org/10.1177/0192623311428473

Dhivya, C., Vandarkuzhali, S. A. A., & Radha, N. (2019). Antimicrobial activities of nanostructured polyanilines doped with aromatic nitro compounds. *Arabian Journal of Chemistry*, *12*(8), 3785–3798. https://doi.org/10.1016/j.arabjc.2015.12.005

EPA, (U.S. (2016). *Drinking Water Health Advisories for PFOA and PFOS* (Issue EPA 800-F-16-003). https://www.epa.gov/sites/default/files/2016-06/documents/drinkingwaterhealthadvisories_pfoa_pfos_updated_5.31.16.pdf. [Access online 21 October 2022].

Fahim, M., Ali Shah, A. ul H., & Bilal, S. (2019). Highly stable and efficient performance of binder-free symmetric supercapacitor fabricated with electroactive polymer synthesized via interfacial polymerization. *Materials*, *12*(10). https://doi.org/10.3390/ma12101626

Faisal, M., Rashed, M. A., Abdullah, M. M., Harraz, F. A., Jalalah, M., & Al-Assiri, M. S. (2020). Efficient hydrazine electrochemical sensor based on PANI doped mesoporous $SrTiO_3$ nanocomposite modified glassy carbon electrode. *Journal of Electroanalytical Chemistry*, *879*. https://doi.org/10.1016/j.jelechem.2020.114805

Faiz, F., Baxter, G., Collins, S., Sidiroglou, F., & Cran, M. (2020). Polyvinylidene fluoride coated optical fibre for detecting perfluorinated chemicals. *Sensors and Actuators, B: Chemical*, *312*. https://doi.org/10.1016/j.snb.2020.128006

Ferrari, A. G. M., Foster, C. W., Kelly, P. J., Brownson, D. A. C., & Banks, C. E. (2018). Determination of the electrochemical area of screen-printed electrochemical sensing platforms. *Biosensors*, *8*(2), 1–10. https://doi.org/10.3390/bios8020053

Figiela, M., Wysokowski, M., Galinski, M., Jesionowski, T., & Stepniak, I. (2018). Synthesis and characterization of novel copper oxide-chitosan nanocomposites for non-enzymatic glucose sensing. *Sensors and Actuators, B: Chemical*, *272*, 296–307. https://doi.org/10.1016/j.snb.2018.05.173

Geetha Devi, M., Shinoon Al-Hashmi, Z. S., & Chandra Sekhar, G. (2012). Treatment of vegetable oil mill effluent using crab shell chitosan as adsorbent. *International Journal of Environmental Science and Technology*, *9*(4), 713–718. https://doi.org/10.1007/s13762-012-0100-4

Goswami, S., Nandy, S., Calmeiro, T. R., Igreja, R., Martins, R., & Fortunato, E. (2016). Stress Induced Mechano-electrical Writing-Reading of Polymer Film Powered by Contact Electrification Mechanism. *Scientific Reports*, *6*. https://doi.org/10.1038/srep19514

Huang, B. H., Li, S. Y., Chiou, Y. J., Chojniak, D., Chou, S. C., Wong, V. C. M., Chen, S. Y., & Wu, P. W. (2021). Electrophoretic fabrication of a robust chitosan/polyethylene glycol/polydopamine composite film for UV-shielding application. *Carbohydrate Polymers*, *273*, 118560. https://doi.org/10.1016/j.carbpol.2021.118560

Karthik, R., & Meenakshi, S. (2015). Adsorption study on removal of Cr(VI) ions by polyaniline composite. *Desalination and Water Treatment*, *54*(11), 3083–3093. https://doi.org/10.1080/19443994.2014.909330

Mittal, H., Ray, S. S., Kaith, B. S., Bhatia, J. K., Sukriti, Sharma, J., & Alhassan, S. M. (2018). Recent progress in the structural modification of chitosan for applications in diversified biomedical fields. *European Polymer Journal*, *109*, 402–434. https://doi.org/10.1016/j.eurpolymj.2018.10.013

Mohd Norsham, I. N., Baharin, S. N. A., Raoov, M., Shahabuddin, S., Jakmunee, J., & Sambasevam, K. P. (2020). Optimization of waste quail eggshells as biocomposites for polyaniline in ammonia gas detection. *Polymer Engineering and Science*, *60*(12), 3170–3182. https://doi.org/10.1002/pen.25545

Mostafaei, A., & Zolriasatein, A. (2012). Synthesis and characterization of conducting polyaniline nanocomposites containing ZnO nanorods. *Progress in Natural Science: Materials International*, *22*(4), 273–280. https://doi.org/10.1016/j.pnsc.2012.07.002

Nontipichet, N., Khumngern, S., Choosang, J., Thavarungkul, P., Kanatharana, P., & Numnuam, A. (2021). An enzymatic histamine biosensor based on a screen-printed carbon electrode modified with a chitosan–gold nanoparticles composite cryogel on Prussian blue-coated multi-walled carbon nanotubes. *Food Chemistry*, *364*, 130396. https://doi.org/10.1016/j.foodchem.2021.130396

Núñez, C., Triviño, J. J., & Arancibia, V. (2021). A electrochemical biosensor for As(III) detection based on the catalytic activity of Alcaligenes faecalis immobilized on a gold nanoparticle–modified screen–printed carbon electrode. *Talanta*, *223,* 121702 . https://doi.org/10.1016/j.talanta.2020.121702

Ordonez, D., Valencia, A., Sadmani, A. H. M. A., & Chang, N. Bin. (2022). Green sorption media for the removal of perfluorooctanesulfonic acid (PFOS) and perfluorooctanoic acid (PFOA) from water. *Science of the Total Environment*, *819*, 152886. https://doi.org/10.1016/j.scitotenv.2021.152886

Padmalaya, G., Vardhan, K. H., Kumar, P. S., Ali, M. A., & Chen, T. W. (2022). A disposable modified screen-printed electrode using egg white/ZnO rice structured composite as practical tool electrochemical sensor for formaldehyde detection and its comparative electrochemical study with Chitosan/ZnO nanocomposite. *Chemosphere*, *288*(P2), 132560. https://doi.org/10.1016/j.chemosphere.2021.132560

Priyanka, S. R., & Latha, K. P. (2021). MnCr2O4 nanocomposite modified carbon paste electrode based electrochemical sensor for determination of Norepinephrine: A cyclic voltammetry study. *Chemical Data Collections*, *35*, 100769. https://doi.org/10.1016/j.cdc.2021.100769

Rajeev, K. K., Kim, E., Nam, J., Lee, S., Mun, J., & Kim, T. H. (2020). Chitosan-grafted-polyaniline copolymer as an electrically conductive and mechanilly stable binder for high-performance Si anodes in caLi-ion batteries. *Electrochimica Acta*, *333*. https://doi.org/10.1016/j.electacta.2019.135532

Ranaweera, R., Ghafari, C., & Luo, L. (2019). Bubble-Nucleation-Based Method for the Selective and Sensitive Electrochemical Detection of Surfactants [Research-article]. *Analytical Chemistry*, *91*(12), 7744–7748. https://doi.org/10.1021/acs.analchem.9b01060

Ryu, H., Li, B., De Guise, S., McCutcheon, J., & Lei, Y. (2021). Recent progress in the detection of emerging contaminants PFASs. *Journal of Hazardous Materials*, *408*, 124437. https://doi.org/10.1016/j.jhazmat.2020.124437

Sahnoun, S., & Boutahala, M. (2018). Adsorption removal of tartrazine by chitosan/polyaniline composite: Kinetics and equilibrium studies. *International Journal of Biological Macromolecules*, *114*, 1345–1353. https://doi.org/10.1016/j.ijbiomac.2018.02.146

Shankar, A., Xiao, J., & Ducatman, A. (2012). Perfluorooctanoic acid and cardiovascular disease in US adults. *Archives of Internal Medicine*, *172*(18), 1397–1403. https://doi.org/10.1001/archinternmed.2012.3393

Suhail, M. H., Abdullah, O. G., & Kadhim, G. A. (2019). Hydrogen sulfide sensors based on PANI/f-SWCNT polymer nanocomposite thin films prepared by electrochemical polymerization. *Journal of Science: Advanced Materials and Devices*, *4*(1), 143–149. https://doi.org/10.1016/j.jsamd.2018.11.006

Sznajder-Katarzyńska, K., Surma, M., & Cieślik, I. (2019). A Review of Perfluoroalkyl Acids (PFAAs) in terms of Sources, Applications, Human Exposure, Dietary Intake, Toxicity, Legal Regulation, and Methods of Determination. *Journal of Chemistry*, *2019*. https://doi.org/10.1155/2019/2717528

Thamilarasan, V., Sethuraman, V., Gopinath, K., Balalakshmi, C., Govindarajan, M., Mothana, R. A., Siddiqui, N. A., Khaled, J. M., & Benelli, G. (2018). Single Step Fabrication of Chitosan Nanocrystals Using Penaeus semisulcatus: Potential as New Insecticides, Antimicrobials and Plant Growth Promoters. *Journal of Cluster Science*, *29*(2), 375–384. https://doi.org/10.1007/s10876-018-1342-1

Waikar, M. R., Rasal, A. S., Shinde, N. S., Dhas, S. D., Moholkar, A. V., Shirsat, M. D., Chakarvarti, S. K., & Sonkawade, R. G. (2020). Electrochemical performance of Polyaniline based symmetrical energy storage device. *Materials Science in Semiconductor Processing*, *120*, 105291. https://doi.org/10.1016/j.mssp.2020.105291

Younis, S. A., Ali, T. A., & Serp, P. (2021). Potential applicability of Zn0.05TiOxNy@MOF-5 nanocomposite for adsorption and electrochemical detection of Zn(II) in saline wastewater. *Journal of Environmental Chemical Engineering*, *9*(5), 106186. https://doi.org/10.1016/j.jece.2021.106186

Zheng, Z., Yu, H., Geng, W. C., Hu, X. Y., Wang, Y. Y., Li, Z., Wang, Y., & Guo, D. S. (2019). Guanidinocalix[5]arene for sensitive fluorescence detection and magnetic removal of perfluorinated pollutants. *Nature Communications*, *10*(1), 1–9. https://doi.org/10.1038/s41467-019-13775-1